Volume 58(7): 595–609, 2010
Journal of Histochemistry & Cytochemistry
http://www.jhc.org

ARTICLE

Variable Expression of Nuclear Receptor Coactivator 4 (NcoA4) During Mouse Embryonic Development

Alexandra Kollara and Theodore J. Brown

Samuel Lunenfeld Research Institute, Mount Sinai Hospital, Toronto, Ontario, Canada, and Department of Obstetrics and Gynecology, University of Toronto, Toronto, Ontario, Canada

SUMMARY Human nuclear receptor coactivator 4 (NcoA4) amplifies the activity of several ligand-activated nuclear transcription factors, including the aryl hydrocarbon receptor (AhR) and androgen receptor (AR). Because these receptors exert important regulatory effects during development, with AhR ubiquitously expressed after embryonic day 9.5 (E9.5) and AR expressed from E12 onward, we examined NcoA4 expression in mouse embryos from E9.5 to E17.5. Full-length NcoA4 transcript was detected by RT-PCR at all embryonic stages and in all adult mouse tissues examined, although a novel splice variant was also detected. Western blot analysis indicated the expression of full-length NcoA4 protein, which was more highly expressed at later (E15.5–E17.5) embryonic stages. NcoA4 protein was also present at varying levels in all adult mouse tissues examined. A dynamic expression profile for NcoA4 during early development was indicated by immunohistochemistry in cardiac, hepatic, and lung tissue. Unlike human NcoA4, murine NcoA4 lacks an LXXLL motif, which has been implicated in the interaction with AR. Overexpression of murine NcoA4 augmented the transcriptional activity of AhR by 5-fold and AR by only 1.5-fold in COS cells. These studies demonstrate ubiquitous NcoA4 expression throughout development and suggest that this coactivator may play a role in modulating nuclear receptor activity, particularly that of the AhR, during development. **(J Histochem Cytochem 58:595–609, 2010)**

KEY WORDS
ARA70
androgen receptor
aryl hydrocarbon receptor
embryo
immunohistochemistry

NUCLEAR RECEPTOR COACTIVATORS modify the transcriptional activity of their targeted receptors by bridging the dimerized receptors with general transcription factors or by affecting receptor folding, stability, or trafficking (Heinlein and Chang 2002). The impact that nuclear receptors have in normal development and disease progression has raised intense interest in the expression and function of coregulators for these receptors. The p160 steroid receptor coactivator family has been the best studied to date, and all three family members have been shown to play important roles in mouse development (Xu and Li 2003).

Nuclear receptor coactivator 4 (NcoA4) is a unique coactivator that interacts with and enhances the transcriptional activity of multiple ligand-activated nuclear receptors, including the androgen receptor (AR), aryl hydrocarbon receptor (AhR), and estrogen, progesterone, glucocorticoid, vitamin D, and peroxisome proliferator-activated α and γ (PPARα/γ) receptors (Yeh and Chang 1996; Gao et al. 1999; Heinlein et al. 1999; Heinlein and Chang 2003; Lanzino et al. 2005; Ting et al. 2005; Kollara and Brown 2006). Expression of this coactivator has been demonstrated in various cell lines and is altered in breast, ovarian, and prostate cancers (Yeh and Chang 1996; Evangelou et al. 2000; Kollara et al. 2001; Shaw et al. 2001; Magklara et al. 2002; Mestayer et al. 2003). A splice variant of human NcoA4 mRNA lacking 985 nucleotides that encodes a protein with an estimated molecular mass of 35 kDa (Alen et al. 1999), which is expressed in some invasive

Correspondence to: Theodore J. Brown, PhD, Samuel Lunenfeld Research Institute, Mt. Sinai Hospital, Box 41, 25 Orde Street, Toronto, ON, Canada M5T 3H7. E-mail: brown@lunenfeld.ca

Received for publication October 26, 2009; accepted March 9, 2010 [DOI: 10.1369/jhc.2010.955294].

ductal carcinomas (Kollara et al. 2001), has also been described in T47D human breast cancer cells.

NcoA4 mRNA is expressed in moderate amounts in different adult rodent tissues, including kidney, heart, lung, stomach, prostate, and brain (Yeh and Chang 1996; Alen et al. 1999; Siriett et al. 2006), with no apparent expression in the cerebral cortex, spleen, or seminal vesicles (Yeh and Chang 1996). The highest level of expression was reported in the testis, which is also the only tissue reported to express an uncharacterized shorter NcoA4 mRNA variant (Alen et al. 1999). The limited available information on the expression of NcoA4 during development is largely focused on male reproductive tissues, because NcoA4 was initially thought to be an AR-specific coactivator (Thin et al. 2002). Our recent discovery of human NcoA4 interaction with the AhR and differential potentiation of AhR transcriptional activity by NcoA4 variants (Kollara and Brown 2006) suggests a broader potential role for this coactivator during development. The AhR is expressed after embryonic day 9.5 (E9.5) in various murine tissues, including the liver, heart, lung, and bone (Abbott et al. 1995; Jain et al. 1998). AhR-null mice display a developmental phenotype including decreased growth rate, peripheral immune system deficiency, heart hypertrophy, and liver and lung fibrosis (Gonzalez et al. 1995; Fernandez-Salguero et al. 1997). AR also plays a well-known role in male differentiation and development and is expressed from E12 onward (Jost et al. 1953; Crocoll et al. 1998). The AR is also expressed in non-reproductive tissues, including the kidney, liver, skeletal muscle, and brain (Keller et al. 1996), and may play a role in the development or function of these tissues as well.

Because NcoA4-interacting nuclear receptors play significant roles during normal development, NcoA4 may exert important regulatory effects on these actions during development and adulthood. To begin to address this hypothesis, we examined the expression of NcoA4 during mouse development. Our results demonstrate a dynamic expression profile for this coactivator during early development, particularly in cardiac, hepatic, and lung tissue. Moreover, we examined the differential effects of mouse NcoA4 on AR and AhR transactivation. These data support the idea that NcoA4 might exert important developmental effects by altering nuclear receptor activity.

Materials and Methods

Animals

Imprinting control region (ICR) mice, originally obtained from Harlan (Indianapolis, IN), were used because these mice are outbred and have a high average litter size of 11.5 compared with other strains. The mice were housed in a controlled environment with a 12-hr light–12-hr dark cycle in the Samuel Lunenfeld Research Institute mouse facility (Toronto, ON, Canada). Females were paired with males, and pregnant females were killed by cervical dislocation on E9.5–E18.5 (considering the day of vaginal plug appearance as E0.5). Embryos were dissected free from the placenta and fetal membranes and were snap-frozen in liquid nitrogen or fixed overnight in 4% paraformaldehyde, pH 7.4, and paraffin-embedded. For studies of adult tissues, ICR mice aged 6–8 weeks were killed by cervical dislocation, and tissues were dissected and frozen in liquid nitrogen. All procedures were approved by the institutional animal care committee (Samuel Lunenfeld Research Institute).

RNA Extraction and RT-PCR

Whole mouse embryos and adult tissue specimens were mechanically homogenized in Trizol reagent (Invitrogen; Burlington, ON, Canada) at 4C. Total RNA was extracted as directed by the manufacturer. RNA concentration was determined spectrophotometrically by measuring absorbance at 260 nm.

Three μg of total RNA were reverse-transcribed using a primer, (5′-TTCACATCTGTAGAGGAGTTC-3′) corresponding to nt 1893–1913 of the murine NcoA4 cDNA sequence (accession number BC085086), and Superscript reverse transcriptase (Invitrogen). The resulting cDNA was amplified using 5′-GCAGAATG-AACACATCCCTGG-3′, corresponding to nt 30–50 of NcoA4, as the forward primer and the above-mentioned oligonucleotide as reverse primer. PCR was performed using Taq polymerase (Fermentas; Burlington, ON, Canada) and involved preincubation at 95C (5 min), followed by denaturation at 94C (90 sec), primer annealing at 55C (75 sec), and extension at 72C (2 min) for 30 cycles. The resulting PCR products were verified by automated nucleotide sequencing.

Western Blot Analysis

Whole mouse embryos and adult tissue specimens were homogenized at 4C in radioimmunoprecipitation assay lysis buffer (150 mM NaCl, 50 mM HEPES, pH 7.25, 1% Triton X-100, 0.1% SDS, 1% sodium deoxycholate) containing Complete protease inhibitor cocktail (Roche Diagnostics; Laval, QC, Canada). Nuclei and cellular debris were removed by centrifugation at 20,000 × g for 15 min at 4C, the clarified lysates were collected, and total protein was quantified (BCA Protein Assay; Pierce, Rockford, IL). Aliquots of lysates containing 20 μg of total protein were subjected to Western blot analysis as described previously (Kollara and Brown 2006) using anti-NcoA4 rabbit polyclonal antibody (H300; 1:200; Santa Cruz Biotechnology, Santa Cruz, CA). Immunoreactive band intensities were quantified using Molecular Dynamics Image Quant version 5.0 software. Western blot analysis

was also performed using anti-NcoA4 goat polyclonal antibodies (Q19 or D19; 1:100; Santa Cruz Biotechnology). Preabsorption of Q19 and D19 antibodies was performed with a 5-fold excess of their respective immunizing peptides (Santa Cruz Biotechnology).

Immunohistochemistry

Microtome sections (4-μm) of paraffin-embedded mouse embryos and adult tissues were subjected to microwave antigen retrieval as described previously (Kollara and Brown 2006). The sections were permeabilized by incubation in PBS containing 0.3% Triton X-100 for 10 min, and endogenous peroxidase was inactivated by incubation in 0.3% H_2O_2 in methanol for 20 min. The sections were blocked by incubation in 10% normal goat serum (NGS; Vector Laboratories, Burlingame, CA) for 1 hr at 22C and then incubated with rabbit anti-NcoA4 antibody (1:200 dilution) in PBS containing 1% NGS overnight at 4C. After washing in PBS, sections were incubated with biotinylated goat anti-rabbit immunoglobulin (IgG) antibody (1:200; Vector Laboratories) in PBS containing 1% NGS for 1 hr, followed by horseradish peroxidase-streptavidin conjugate (1:400; Vector Laboratories) in PBS for 30 min. To visualize staining, the sections were incubated with 0.07% 3,3-diaminobenzidine (Sigma; St. Louis, MO) and 0.03% H_2O_2 in PBS for 12 min and counterstained with hematoxylin (Sigma). Three independent experiments with six embryos in each experiment were run for E9.5 to E13.5 and with two embryos per experiment for E14.5 to E17.5. Immunohistochemical analysis was also performed using anti-NcoA4 goat polyclonal antibodies (Q19 or D19; 1:100; Santa Cruz Biotechnology). Preabsorption studies were performed with Q19 antibody preincubated with a 5-fold molar excess of the immunizing peptide (Santa Cruz Biotechnology).

NcoA4 Expression Constructs

An expression construct for full-length murine NcoA4 (pcDNA3-mNcoA4) was generated by ligating a 3352-bp EcoRI/NotI digest from pCMV-SPORT6.1.ccdb–NcoA4 cDNA [American Type Culture Collection (ATCC), Manassas, VA] into the EcoRI/NotI site of pcDNA3 (Invitrogen). The resulting pcDNA3-mNcoA4 construct was verified by automated nucleotide sequencing. Full-length mouse AhR (pcDNA3-AhR) cDNA was provided by Dr. O. Hankinson (University of California, Los Angeles) and human AR (pcDNA3-AR) cDNA was generated as previously described (Kollara and Brown 2009).

Cell Culture

COS cells (ATCC) were grown in DMEM supplemented with 10% heat-inactivated charcoal-stripped FBS, 100 U/ml penicillin, and 100 μg/ml streptomycin (all from Gibco-BRL; Gaithersberg, MD) at 37C in a humidified CO_2 incubator. 2,3,7,8-Tetrachlorodibenzo-*p*-dioxin (TCDD) dissolved in *n*-nonane was obtained from Cambridge Isotope Laboratories, Inc. (Andover, MA), and 5α-androstan-17β-ol-3-one [dihydrotestosterone (DHT)] was obtained from Sigma and dissolved in ethanol; both compounds were diluted with culture medium before addition to cell cultures. Vehicle treatments consisted of an equivalent amount of *n*-nonane/ethanol diluted with culture medium.

Reporter Gene Studies

COS cells seeded into 24-well plates at a density of 5×10^4 cells/well were transiently transfected with the AR-responsive reporter construct MMTV-luciferase or the AhR-responsive construct pGudluc6.1 (provided by Dr. M.S. Denison, University of California, Davis). Cells were cotransfected with pcDNA3-mNcoA4, pcDNA3-AR, or pcDNA3-AhR as indicated in the Results section using Lipofectamine 2000 (Invitrogen) according to the manufacturer's recommended protocol. The total amount of plasmid DNA used was normalized to 0.8 μg/well by the addition of empty vector. The transfected cells were treated with 10 nM DHT, 10 nM TCDD, or vehicle (final concentration 0.001% ethanol or 0.0064% *n*-nonane) 24 hr after transfection and harvested 24 hr later. Cell lysates were prepared using reporter lysis buffer (Promega; Madison, WI) according to the manufacturer's recommended protocol, and luciferase activity was measured using a Micro-Lumat Plus LB96V luminometer (EG&G Berthold; Oak Ridge, CA).

Luciferase activity was normalized to β-galactosidase activity, measured as described by Sambrook and Russell (2001), to account for minor differences in transfection efficiency. All treatment transfections were performed in triplicate, and each experiment was independently repeated three times.

Statistical Analysis

Normalized data are expressed as the mean fold change (±SEM) relative to that measured in vehicle-treated cells transfected with empty expression vector alone and were analyzed using two-way ANOVA followed by Fisher's least significant difference post-hoc test ($p<0.05$; SPSS v.11 statistical software, Chicago, IL).

Results

NcoA4 mRNA Expression During Embryonic Development and in Adult Tissues

RNA isolated from E9.5–E18.5 embryos was subjected to RT-PCR using primers specific for NcoA4. Two PCR products migrating at 1.9 kb and 1.2 kb were detected (Figure 1A). To determine NcoA4 transcript

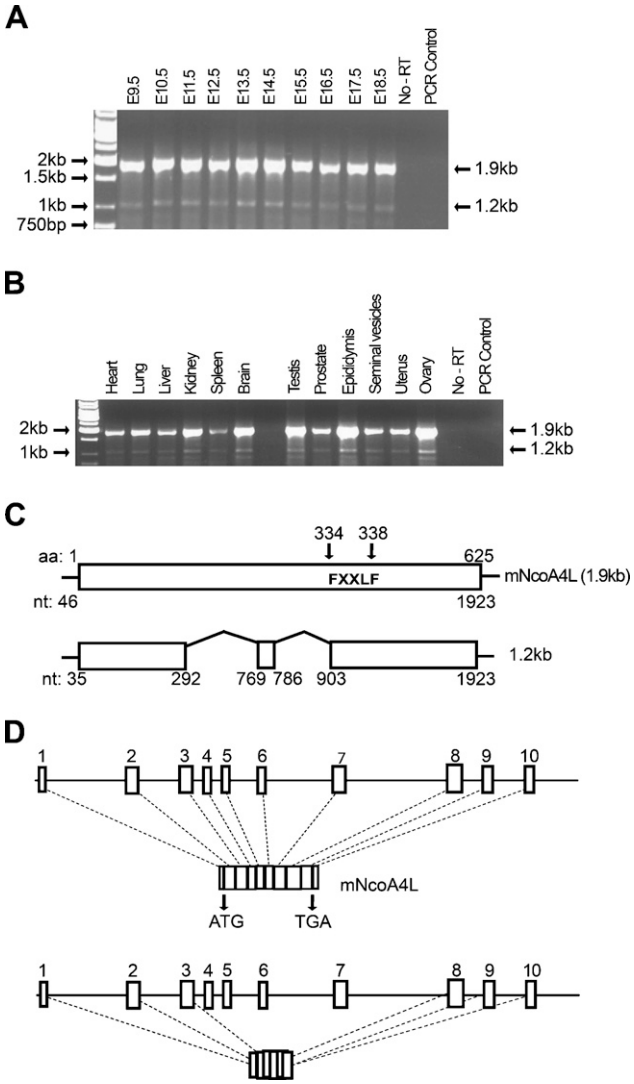

Figure 1 Nuclear receptor coactivator 4 (NcoA4) mRNA expression during mouse development and in different adult mouse tissues. Total RNA was extracted from homogenized embryonic day 9.5 (E9.5) to E18.5 whole mouse embryos (**A**) and from various adult mouse tissues (**B**), and RT-PCR was performed. Two PCR products migrating at 1.9 and 1.2 kb were detected. Automated nucleotide sequencing confirmed that the higher band corresponds to the published full-length mouse NcoA4 cDNA consisting of 1923 nucleotides (mNcoA4), whereas the lower band lacks 588 nucleotides (missing nt 293–768 and nt 787–898) (**C**). The NcoA4 protein contains the FXXLF signature motif at aa 334–338 (**C**). Alignment of these sequences with mouse chromosome 14 using Ensembl Mouse Genome Browser software indicated that murine NcoA4 consists of 10 exons, whereas the 1.2-kb mRNA excludes exons 4, 5, 6, and 7, and portions of exons 3 and 8 (**D**).

expression in adult tissues, a panel of mouse tissues was also examined by RT-PCR. Consistent with the embryo expression, two PCR products migrating at 1.9 kb and 1.2 kb were detected in all tissues examined (Figure 1B). The PCR products were further verified by automated nucleotide sequencing. BLAST analysis (http://www.ncbi.nlm.nih.gov/BLAST/) of the sequences confirmed that they represent mouse NcoA4 cDNA. The 1.9-kb product was identical to the published full-length mouse NcoA4 cDNA sequence (accession number BC085086), whereas the 1.2-kb product lacks 586 nucleotides (missing nt 293–768 and 787–898). The murine NcoA4 protein sequence contains the FXXLF motif (where F = phenylalanine, X = any amino acid, and L = leucine) at aa 334–338 but not the LXXLL signature motif for nuclear receptor coactivators found in the human sequence. Using Ensembl Mouse Genome Browser software (http://www.ensembl.org/), we predicted that the full-length mouse NcoA4 gene, located at chromosome 14A3, would consist of 10 exons, whereas the short 1.2-kb product would lack exons 4, 5, 6, and 7 and portions of exons 3 and 8 (Figure 1D).

NcoA4 Protein Expression During Embryonic Development and in Adult Tissues

Total protein was isolated from whole mouse embryos, and the expression of NcoA4 protein during embryogenesis was determined by Western blot analysis. An immunoreactive band with an estimated molecular mass of 70 kDa was detected with highest intensity in E15.5 to E17.5 embryos (Figure 2A). This immunoreactive band was nearly undetectable at earlier developmental ages (Figure 2A). A 70-kDa immunoreactive band was detected in all adult tissues examined (Figure 2B), with highest intensity in cardiac tissue and least intensity in brain and seminal vesicles (Figure 2B). A highly intense immunoreactive band of lower apparent molecular mass (~55 kDa) was also detected throughout embryonic development (Figure 2A) and with varying intensity in almost all adult tissues examined (Figure 2B).

The 55-kDa band does not correspond to the estimated molecular mass of the product of the 1.2-kb transcript detected by RT-PCR; however, it is possible that it may represent an additional NcoA4 isoform. A 55-kDa immunoreactive band was also detected in some adult tissues, and although this may represent degradation products, it is important to note that the 55-kDa band was observed with three other NcoA4 antibodies: a rabbit polyclonal antibody raised against aa 466–480 (Sigma), a goat polyclonal antibody raised against aa 275–325 (Q19), and a goat polyclonal antibody raised against aa 41–60 (D19). Western blot analysis using two goat polyclonal antibodies (Q19 and D19) preabsorbed with their corresponding immunizing peptides indicated decreased staining of both the 70-kDa and 55-kDa bands, which supports the idea that both bands represent NcoA4-like immunoreactivity (Figure 3).

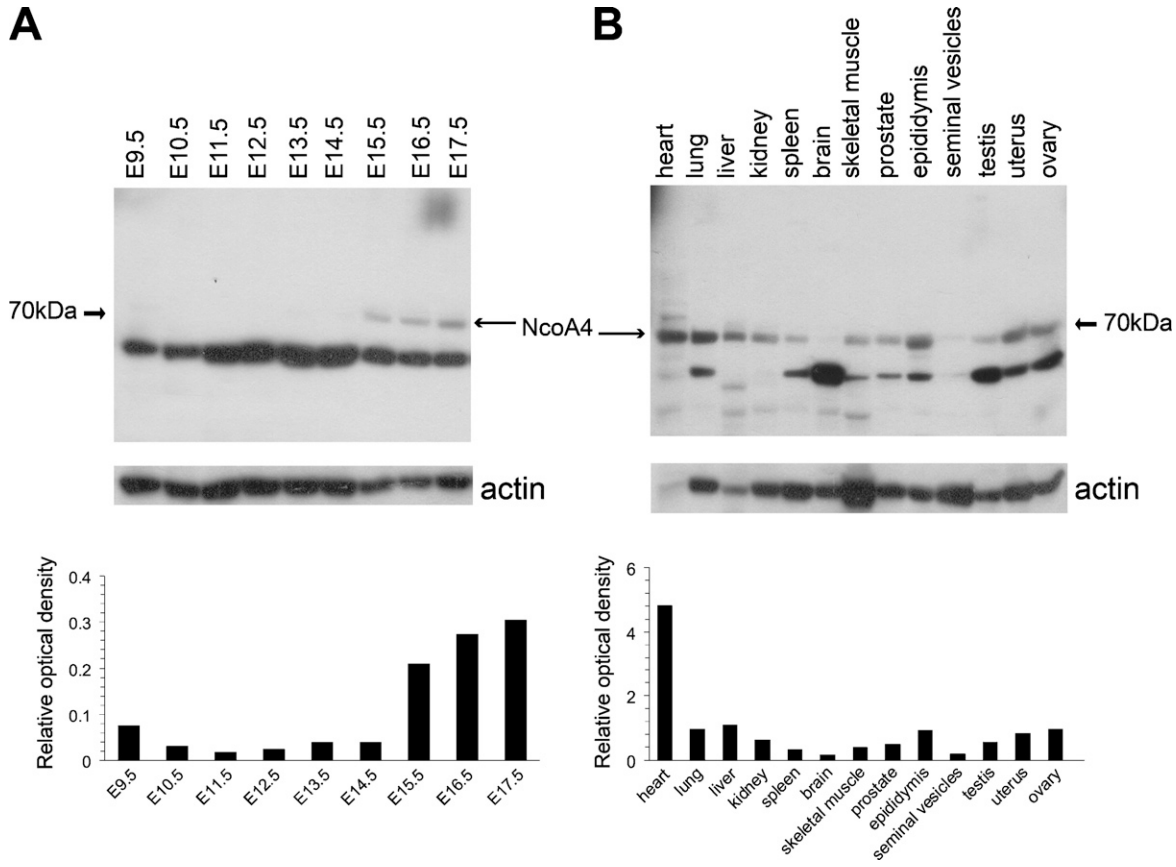

Figure 2 NcoA4 protein expression during mouse development and in different adult mouse tissues. Total protein was extracted from homogenized E9.5–E17.5 whole mouse embryos and from various adult mouse tissues, and Western blot analysis for NcoA4 expression was performed. A 70-kDa immunoreactive band was detected at the later stages (E15.5–E17.5) of embryonic development (**A**). A 70-kDa immunoreactive band was also detected in all the adult tissues examined (**B**). NcoA4 protein levels were normalized using actin protein as a loading control. Representative blots are shown (**A,B**). The bar graphs summarize the results of these experiments expressed as the ratio of the 70-kDa intensity relative to actin.

Two in-frame potential downstream alternate start sites are present in the murine NcoA4 sequence that could result in a protein of ~51 or 59 kDa. However, these correspond to amino acid residues 96 and 167 of the full-length protein and are not likely to explain the 55-kDa immunoreactive protein, because the band was also detected with D19 antibody, which was raised against amino acid residues 40–61. It remains possible that the 55-kDa protein may represent a protein product from a unique splice variant transcript.

Immunohistochemical Localization of NcoA4 Protein During Embryonic Development

The tissue distribution of NcoA4 protein in paraffin-embedded mouse embryo sections was examined by immunohistochemistry using the H300 or Q19 antibody. NcoA4-immunoreactive protein was highly expressed in embryonic heart, liver, lung, cartilage, and other tissues such as brain and somites. Within cardiac tissue, NcoA4 immunoreactivity obtained with H300 was detected in the ventricular cardiomyocytes, with greater intensity observed from E11.5 to E13.5 (Figure 4A). A similar but less-intense staining pattern was observed in cardiac tissue with the Q19 antibody (Figure 4B). A biphasic pattern of expression was revealed in hepatic tissue. High levels of staining obtained with H300 were observed at E12.5, E16.5, and E17.5, with lower intensity staining observed at E10.5 and E11.5, and at E13.5 to E15.5 (Figure 5A). A similar pattern was observed with Q19 antibody (Figure 5B). NcoA4 staining obtained with H300 in the mouse embryo lung bronchioles was of high intensity from E12.5 to E14.5 and was almost undetectable at later stages (E15.5 to E17.5) (Figure 6A). Less-intense staining was observed with Q19; however, higher levels of staining were observed from E12.5 to E14.5 (Figure 6B), consistent with the pattern shown with H300. In all three tissues, cardiac, hepatic, and lung, the staining was predominantly cytoplasmic.

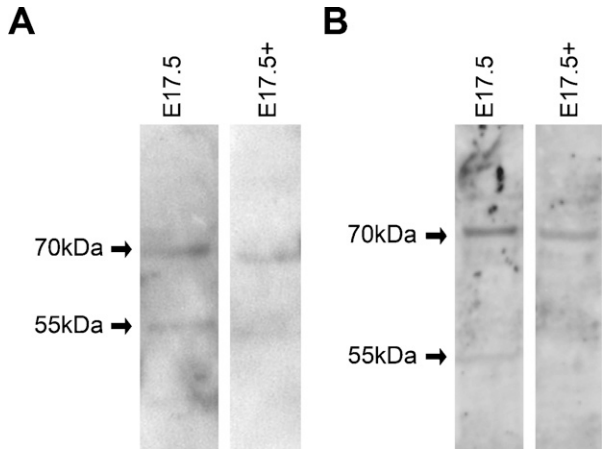

Figure 3 Western blot analysis using NcoA4 antibody preabsorbed with the immunizing peptide. Western blot analysis was performed using whole mouse E17.5 lysates with anti-NcoA4 antibodies Q19 (**A**) or D19 (**B**) or antibodies preabsorbed with their respective immunizing peptides (E17.5+). Decreased expression of both the 70-kDa and 55-kDa immunoreactive bands was observed.

The specificity of the NcoA4 staining was verified by performing immunohistochemical staining on adult mouse ovary using primary antibody (Q19) preabsorbed with the immunizing peptide, because competing peptide is not available for H300. No staining was detected with the preabsorbed antibody (Figure 6C).

To further determine tissue-specific expression of NcoA4, protein lysates of cardiac and hepatic tissue dissected from E14.5 and E17.5 embryos were subjected to Western blot analysis. Whereas a 70-kDa immunoreactive protein was detected in cardiac lysates from both embryonic stages, a differential expression of NcoA4 was found in hepatic tissue: the 70-kDa immunoreactive band, consistent with full-length NcoA4, was predominant at E17.5 (Figures 7A and 7B). This expression is consistent with our immunostaining results (Figure 5) and further verifies the specificity of our NcoA4 antibody. Similar results were obtained using the other three NcoA4 antibodies (data not shown).

Tissue Distribution of NcoA4 Protein in Adult Mouse Tissues

Immunohistochemical staining of adult mouse tissues for NcoA4 using H300 and Q19 revealed ubiquitous expression in both reproductive and non-reproductive tissues. In male reproductive organs, intense nuclear and cytoplasmic staining was observed in testicular Sertoli cells, spermatagonia, spermatocytes, and spermatids, whereas interstitial Leydig cells exhibited less-intense staining (Figures 8 and 9). In the prostate gland, NcoA4 protein was predominantly expressed in the cytoplasm of glandular epithelial cells, with little or no NcoA4 staining detected in the stroma. High levels of NcoA4 staining were detected in columnar epithelial cells of the epididymis, whereas the layer of smooth-muscle cells surrounding the ducts was negative. A similar pattern was observed in the seminal vesicles, with staining observed in the columnar epithelial cells and a lack of staining in the muscular wall (Figures 8 and 9).

In female reproductive tract tissues, intense NcoA4 immunoreactivity was detected in ovarian granulosa cells, thecal cells, and oocytes (Figures 8 and 9). High levels of staining were also noted in corpora lutea (not shown). Little or no staining was observed in the ovarian stroma. In the uterus, intense NcoA4 staining was detected throughout the endometrium, most notably in glandular epithelium. Little or no staining was noted in the circular smooth-muscle layer (Figures 8 and 9).

Also examined were other adult mouse tissues, such as heart, lung, liver, spleen, kidney, and skeletal muscle (Figures 8 and 9). Less-intense NcoA4 staining was detected in the adult heart, as compared with the developing heart (Figures 8 and 9 vs Figure 4). In the adult lung, the epithelial cells of the bronchioles and the alveoli were stained positive, whereas the smooth-muscle cells of the bronchioles were negative for NcoA4 staining. In the liver, overall NcoA4 staining was weak, with occasional hepatocytes showing positive staining. Intense NcoA4 staining was detected in adult mouse spleen, with both the red and white pulp showing expression. Intense nuclear and cytoplasmic staining was detected in cells of the renal tubules, with less-intense staining detected in the cells of the proximal tubules. The skeletal muscle fibers were also stained positive for NcoA4 protein, whereas the flattened nuclei at the periphery of the fibers were negative (Figures 8 and 9).

Overexpression of NcoA4 Amplifies AR and AhR Activity

To determine whether murine NcoA4 is able to amplify AR or AhR activity, the effect of overexpression of mNcoA4 on receptor transcriptional activity was examined. COS cells were transiently transfected with a luciferase reporter construct containing an androgen- or dioxin-responsive promoter and varying amounts of an expression construct for mNcoA4. Twenty-four hr after transfection, cells were treated with DHT, TCDD, or vehicle (control), and they were harvested 24 hr later for luciferase activity determination.

Transfection of mNcoA4 resulted in a dose-dependent increase in AR-dependent luciferase expression induced by DHT (Figure 10A). At the highest amount of transfected mNcoA4, a >50% increase in luciferase activity was observed, as compared with that of DHT-treated

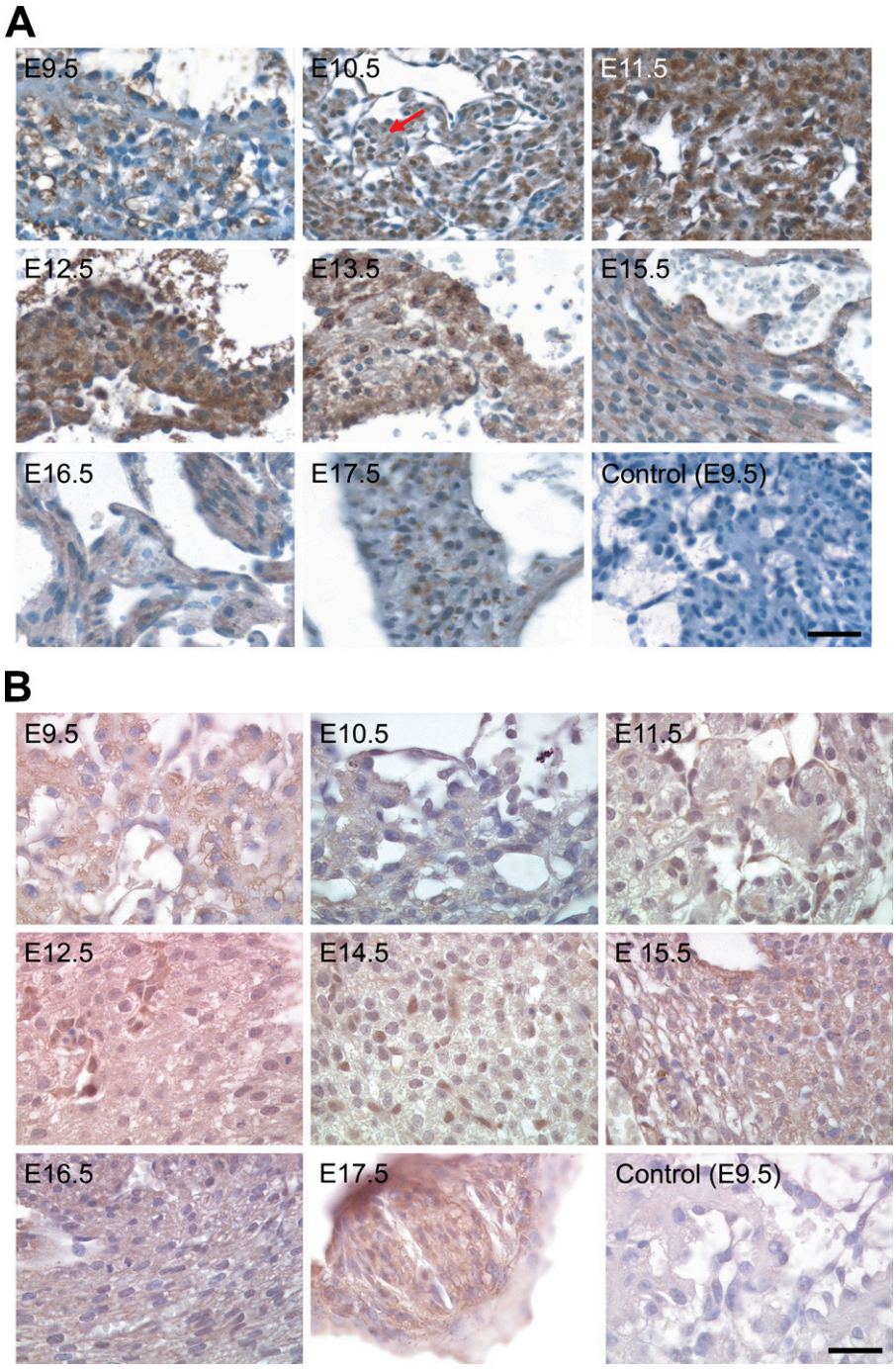

Figure 4 NcoA4 protein distribution in cardiac tissue during mouse development. Tissue distribution of NcoA4 protein in paraffin-embedded mouse embryo sections was determined by immunohistochemistry using rabbit anti-NcoA4 H300 (**A**) or goat anti-NcoA4 Q19 (**B**) polyclonal antibodies. All sections were counterstained with hematoxylin. NcoA4 immunoreactivity obtained with H300 was detected in ventricular cardiomyocytes (red arrow), with greater intensity observed from E11.5 to E13.5 (**A**). A similar but less-intense staining pattern was observed in cardiac tissue with the Q19 antibody (**B**). Absence of primary antibody or nonspecific IgG was used as a negative control, as shown for E9.5. Bars: **A** = 40 μm; **B** = 25 μm.

cells transfected with empty expression vector. mNcoA4 did not affect luciferase expression in the absence of ligand. Transfection of mNcoA4 resulted in a 5-fold increase in AhR-dependent luciferase expression induced by TCDD (Figure 10B), as compared with TCDD-treated cells transfected with empty expression vector. This effect of mNcoA4 was achieved after transfection with the highest amount (500 ng) of cDNA, whereas lower amounts increased AhR transcriptional activity by only 40–50%. A small but statistically significant increase in luciferase expression by mNcoA4 transfection was noted in the absence of TCDD treatment, consistent with the possible presence of an endogenous AhR ligand.

Discussion

The ubiquitous expression of NcoA4 mRNA and protein during early mouse embryo development, with

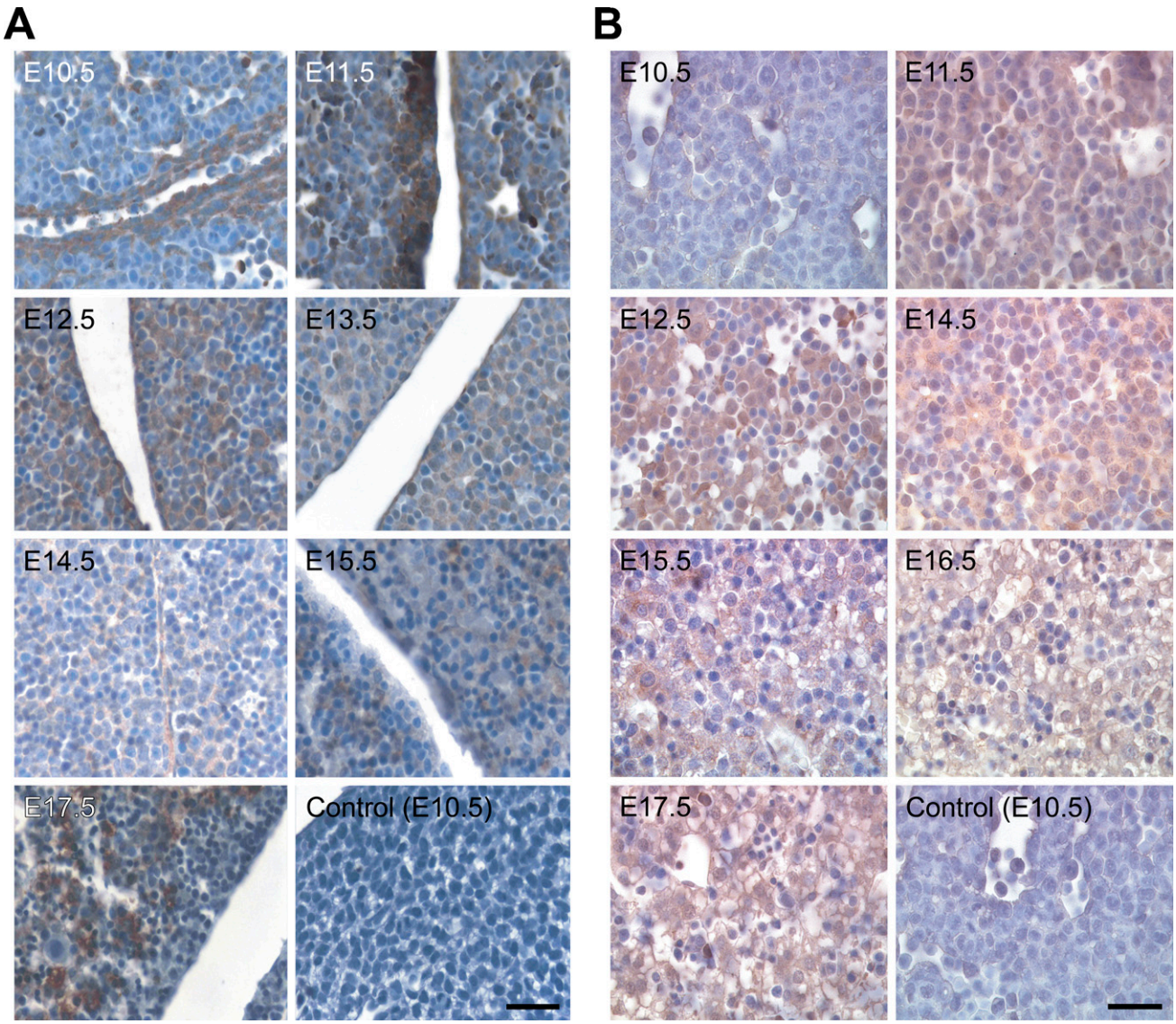

Figure 5 NcoA4 protein distribution in hepatic tissue during mouse development. Tissue distribution of NcoA4 protein in paraffin-embedded mouse embryo sections was determined by immunohistochemistry using rabbit anti-NcoA4 H300 (**A**) or goat anti-NcoA4 Q19 (**B**) polyclonal antibodies. All sections were counterstained with hematoxylin. The two compartments shown in **A** are two lobes of the liver. NcoA4 protein was expressed with high intensity in the hepatic tissue of the mouse embryo at E12.5 and E17.5, and less-intense NcoA4 staining was detected at E10.5 and E11.5 and from E13.5 to E15.5. Absence of primary antibody or nonspecific IgG was used as a negative control, as shown for E10.5. Bars: **A** = 40 μm; **B** = 25 μm.

intense expression in cardiac, hepatic, and lung tissue, is demonstrated in this study. Our data further demonstrate ubiquitous NcoA4 mRNA and protein expression in adult mouse tissues. The impact of overexpression of full-length murine NcoA4 on AR and AhR signaling suggests that murine NcoA4 may function more as a coactivator for AhR than AR.

Murine NcoA4 contains a conserved FXXLF motif but lacks an LXXLL motif, both of which are present in human NcoA4 (Heinlein et al. 1999; Zhou et al. 2002). The FXXLF motif of human NcoA4 is involved in AR interaction, whereas the LXXLL motif is involved in PPARγ and vitamin D receptor interaction (Heinlein et al. 1999; Zhou et al. 2002; Ting et al. 2005). Neither motif appears essential for human NcoA4 coactivator function with AhR (Kollara and Brown 2006). The presence of different motifs between mouse and human NcoA4 suggests differences in the interaction with different receptors and possibly differences in modulation of receptor action between species (human vs mouse). To our knowledge, there are no previous studies examining nuclear coactivator func-

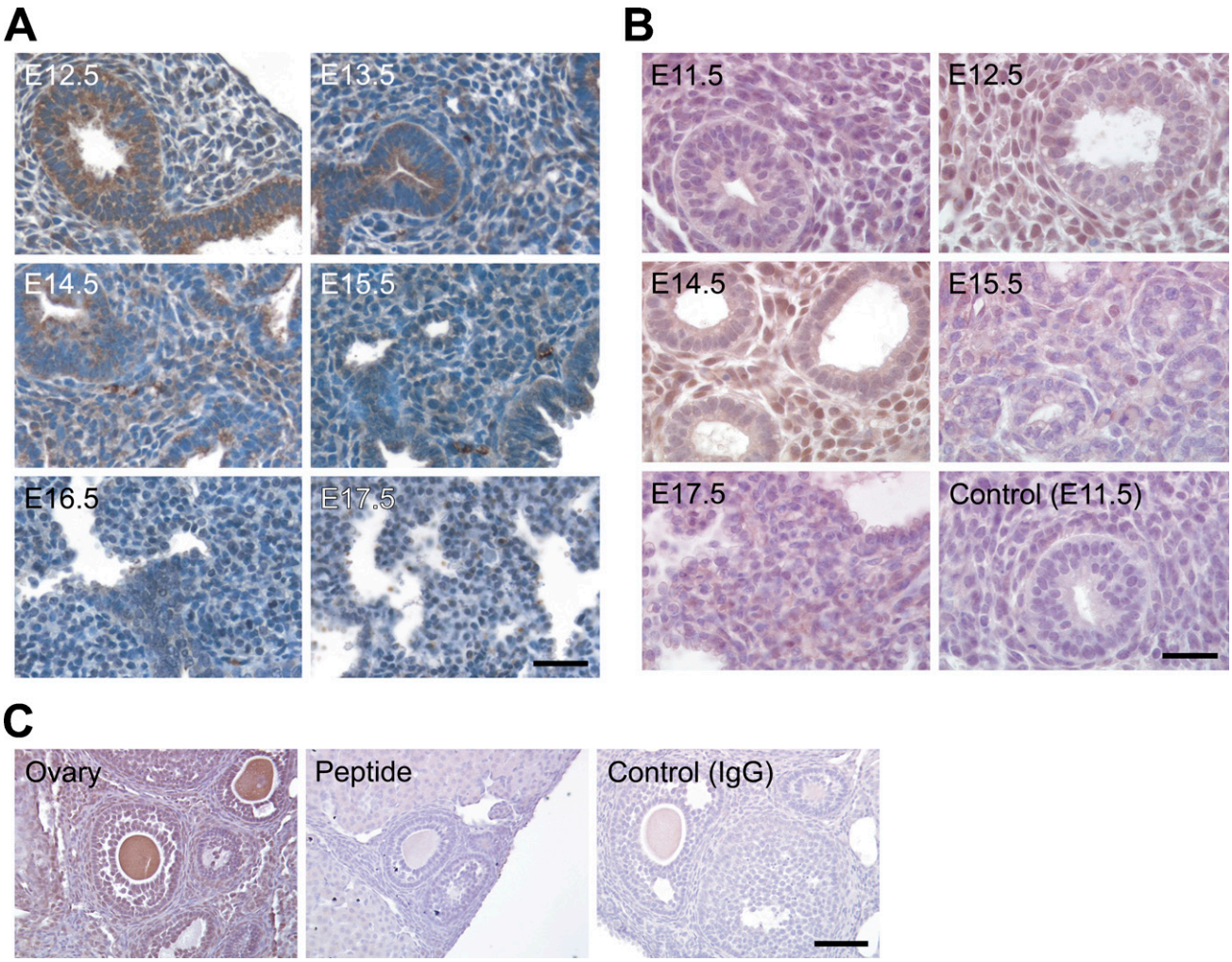

Figure 6 NcoA4 protein distribution in lung tissue during mouse development and preabsorption with the corresponding immunizing peptide on adult mouse ovary. Tissue distribution of NcoA4 protein in paraffin-embedded mouse embryo sections was determined by immunohistochemistry using two NcoA4 antibodies; the rabbit H300 (**A**) or the goat Q19 (**B**) polyclonal antibody. All sections were counterstained with hematoxylin. Whereas high-intensity NcoA4 staining was detected in the mouse embryo lung at E12.5 to E14.5, NcoA4 staining at E15.5 to E17.5 was nearly undetectable. Staining with normal goat serum substituted for primary antibody was used as negative control and is shown for E11.5. Immunostaining with the Q19 antibody preabsorbed with the corresponding immunizing peptide was also performed (**C**). Bars: **A** = 40 μm; **B,C** = 25 μm.

tion of murine NcoA4. We demonstrate here that murine NcoA4 is a potent coactivator for AhR, exhibiting a greater fold-induction effect (5-fold) on TCDD-induced DRE-luciferase expression than what we have reported for human NcoA4 (3-fold) (Kollara and Brown 2006). In contrast, murine NcoA4 appears to be less effective in amplifying AR activity (1.5-fold) than human NcoA4 determined using MMTV-luciferase (3-fold) (data for human NcoA4 not shown). The lower efficacy of murine NcoA4 for AR transactivation observed may reflect the fact that human rather than murine AR was used for the AR coactivator studies. However, the region of the ligand-binding domain (aa 698–720) of the wild-type human AR thought to mediate NcoA4 interaction (Alen et al. 1999; Zhou et al. 2002; Hu et al. 2004) is identical in amino acid sequence with murine AR (accession number BC132975 vs X53779).

The regions of human NcoA4 involved in modulating AR coactivator function are loosely defined. Although the FXXLF motif interacts with the ligand-binding domain of the AR (He et al. 2002; Zhou et al. 2002; Hu et al. 2004), other regions of the protein have been implicated as enhancers or repressors of its AR coactivator function. Zhou et al. (2002) have indicated that a centrally located region of NcoA4, referred to as the activation domain and consisting of more than the FXXLF motif, enhances AR transactivation. Similarly, the N-terminal region of NcoA4, which contains a coiled-coil domain, is

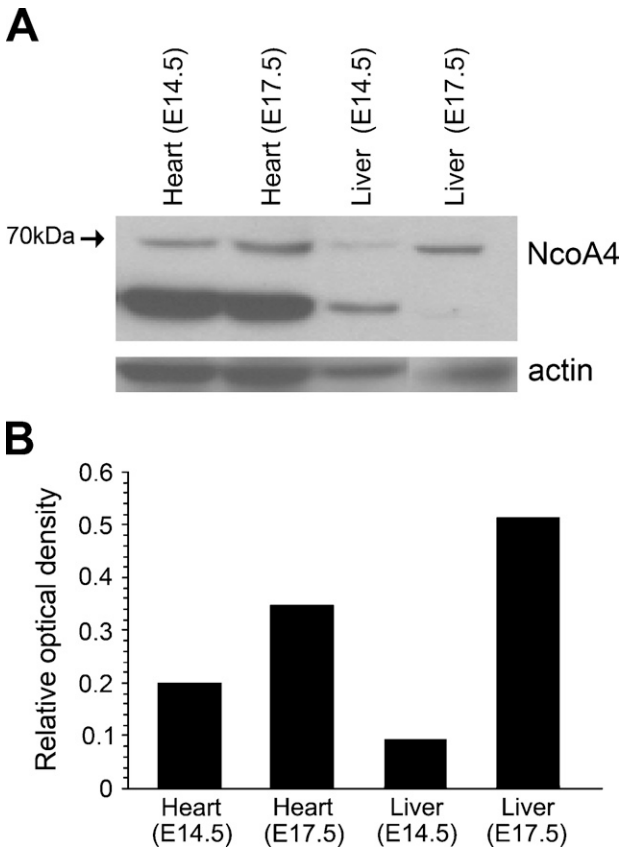

Figure 7 NcoA4 protein expression in cardiac and hepatic tissue at E14.5 and E17.5. Total protein was extracted from E14.5 and E17.5 whole heart and liver and was subjected to Western blot analysis using rabbit polyclonal NcoA4 antibody. A 70-kDa immunoreactive band and a 55-kDa immunoreactive band were detected in the cardiac tissue at both embryonic stages, and a differential expression of the 70-kDa immunoreactive band was observed in the hepatic tissue. A representative blot is shown (**A**). The bar graph summarizes the results of this experiment expressed as the ratio of 70-kDa protein normalized to actin protein used as a loading control (**B**).

essential for enhancing AR transcriptional activity, but is not required for the NcoA4–AR interaction (Hu et al. 2004). In contrast, the C-terminal region of human NcoA4 (aa 499–614) may harbor elements that decrease the ability of NcoA4 to function as an AR coactivator (Thin et al. 2002; Rahman et al. 2003).

BLAST analysis performed on the sequence of the shorter RT-PCR product (1.2 kb) identified in this study aligned with full-length NcoA4, but lacked a total of 588 nucleotides (nt 293–768 and 787–898). Submission of this sequence to ExPASy suggests that this transcript may be translated as two different protein products. If the transcript is read from the same start codon as full-length NcoA4, the transcript would generate a truncated protein of only 13 kDa because of an early stop codon introduced as a result of the presumed alternate splicing. However, if a downstream initiation site were used, a translated protein of ~38 kDa molecular mass is predicted, which would include aa 289–625 of the full-length protein sequence. The primary antibody used throughout this study was generated against the first 300 amino acids of full-length NcoA4 and thus would probably not detect this 38-kDa isoform. A 13-kDa immunoreactive band was not detected in our Western blot analysis.

Recently, Siriett et al. (2006) demonstrated the expression of a short murine NcoA4 transcript variant by performing suppressive subtraction hybridization on cDNA generated from C57BL/10 mouse biceps femoris muscle. This variant is identical to the full-length variant but would encode a protein with a nine consecutive amino acid deletion and six amino acid substitution at the C terminus. The functional significance of this variant has not been explored. The experimental approach used in the present study would not have detected expression of this variant, and we cannot exclude the expression of this or additional NcoA4 variants during development.

Although NcoA4 transcripts are expressed throughout embryo development (E9.5 to E17.5), a differential expression pattern was observed at the protein level. Full-length NcoA4 protein was nearly undetectable at early embryonic stages (E9.5 to E14.5). In contrast, RT-PCR indicated expression of NcoA4 transcript at all stages; however, it is important to note the PCR

Figure 8 NcoA4 protein distribution in various adult mouse tissues. Tissue distribution of NcoA4 protein on paraffin-embedded adult mouse tissue sections was determined by immunohistochemistry using anti-NcoA4 rabbit H300 polyclonal antibody. All sections were counterstained with hematoxylin. NcoA4 protein was highly expressed in testicular Sertoli cells (black arrow) and at all stages of spermatogenesis, whereas little staining was observed in Leydig cells (inset). In the prostate gland, glandular epithelial cells were stained positive, (thick red arrow), whereas staining was absent in the surrounding stroma (black arrow). Intense NcoA4 protein staining was detected in the columnar epithelial cells of the epididymis (red arrow). The columnar epithelial cells of the seminal vesicles were stained positive for NcoA4 (white arrow), whereas staining was absent in the muscular wall surrounding the lumen. NcoA4 protein was highly expressed in oocytes, granulosa cells (white arrow), and thecal cells surrounding the follicle (black arrow). However, the surrounding ovarian stroma was negative for NcoA4. Intense NcoA4 staining was detected in the glands of the uterus (white arrow), whereas little or no staining was detected in the circular (red arrow) smooth-muscle layer. NcoA4 protein was expressed in cardiac muscle but with less intensity than in the heart of the developing embryo. In the adult lung, both the bronchioles (black arrow) and alveoli (red thick arrow) stained positive for NcoA4 expression. Weak staining was detected in the liver, and strong staining was observed in the spleen. In the kidney, an intense staining for NcoA4 was detected in the distal ducts (black arrow) with less-intense staining in the proximal ducts (thick red arrow). Skeletal muscle fibers were positive (white arrow) for NcoA4, whereas the nuclei at the periphery of the fibers (red arrow) were negative. Staining in the absence of primary antibody was used as negative control for all tissues examined (not shown). Bar = 40 μm.

The Journal of Histochemistry & Cytochemistry

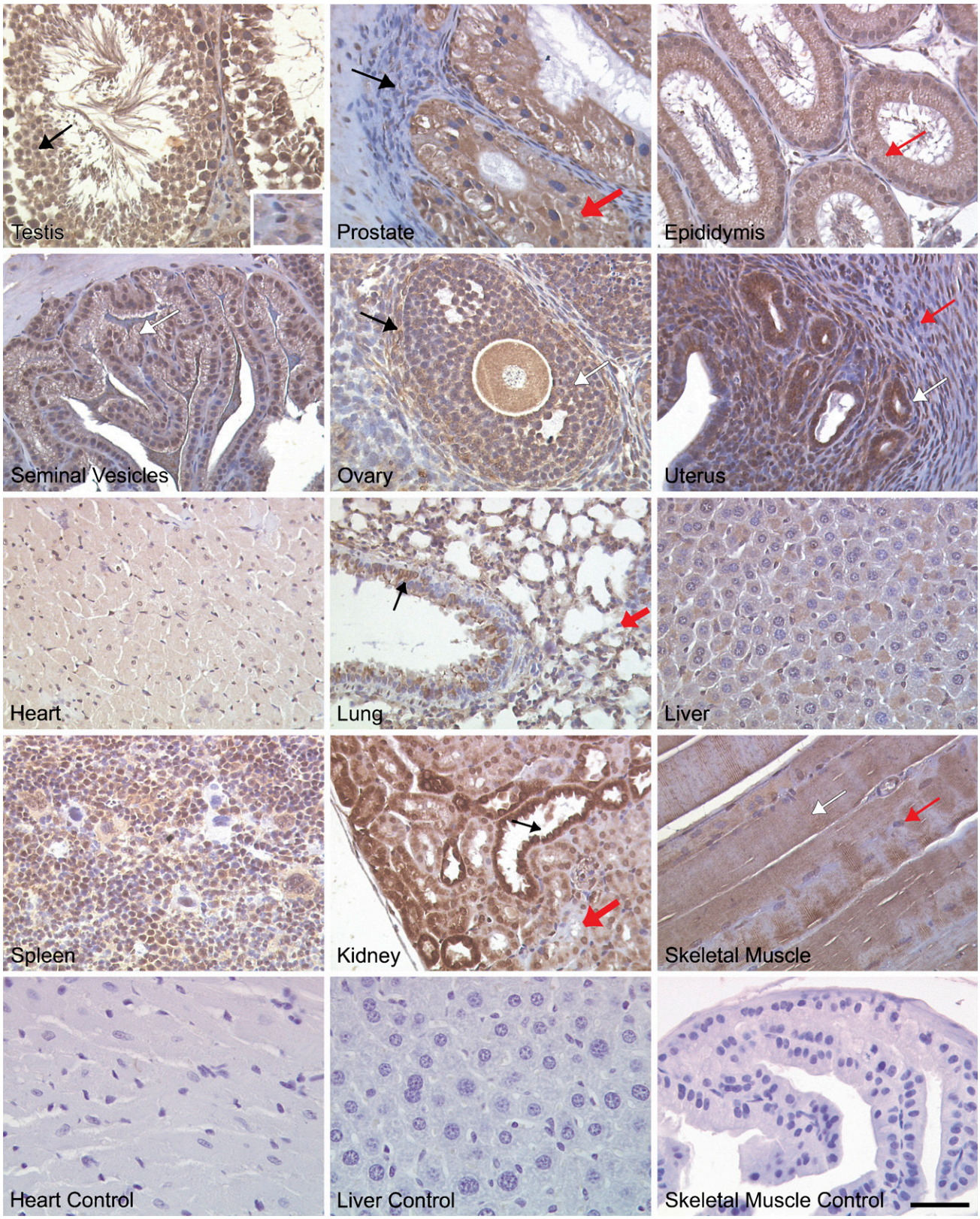

The Journal of Histochemistry & Cytochemistry

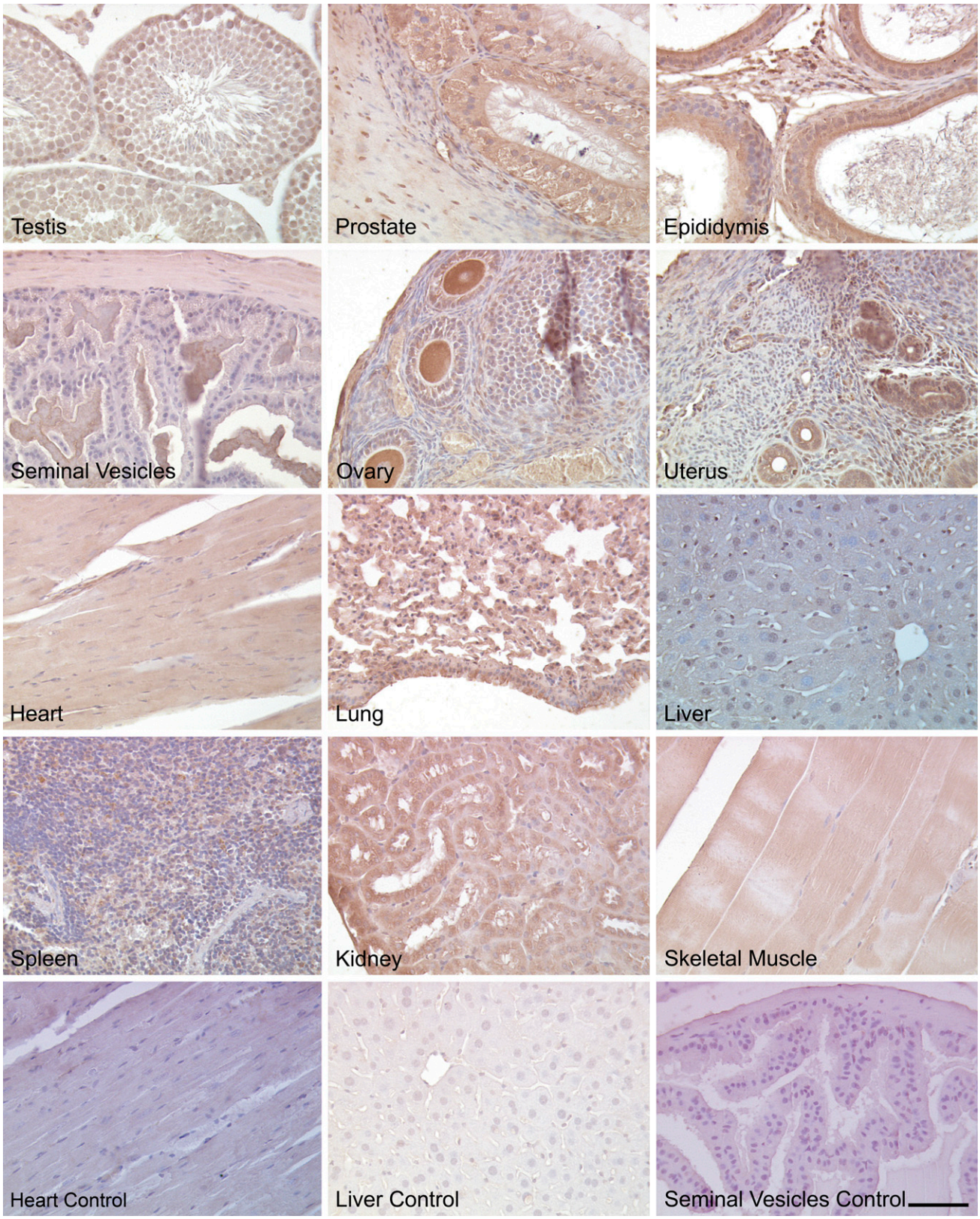

conducted was qualitative rather than quantitative. Full-length NcoA4 protein expression was detected when whole embryo Western blots were exposed to film for an increased period of time at these embryonic stages. The expression of protein at these time points is further evidenced by immunohistochemical analysis for NcoA4 in heart, liver, and lung, as shown in Figures 4–6.

Our immunohistochemistry indicates that NcoA4 protein is mainly expressed in the cell cytoplasm. Several p160 coactivators have also been shown to localize to both the cell cytoplasm and nucleus and to shuttle between the cytoplasmic and cell nuclear compartments, owing to the presence of an N-terminal nuclear localization signal and a C-terminal domain region involved in nuclear export (Amazit et al. 2003,2007). However, absence of these domains in NcoA4 suggests that NcoA4 may act differently from the p160 coactivators, leading to speculation that NcoA4 may be involved in receptor folding, receptor stabilization, initial binding events, or other functional roles that need to be further explored.

A dynamic expression profile for NcoA4 was observed in cardiac, hepatic, and lung embryonic tissue. Although more-intense NcoA4 protein staining was detected at early embryonic stages, as compared with later stages in cardiac and lung tissue, fluctuating levels of NcoA4 staining were observed among the different embryonic stages in hepatic tissue. A shift in expression of NcoA4 observed in the liver at E14.5, as opposed to E17.5, may reflect the relative number of hematopoietic cells present in the extract. Hepatic embryonal hematopoesis occurs after E11, with erythroblasts at various stages of maturation present until E15 (Sasaki and Matsumura 1986). Our results indicate low levels of NcoA4 expression in the adult mouse liver, consistent with the study by Siriett et al. (2006), which demonstrated NcoA4 mRNA expression by in situ hybridization. In contrast, Yeh and Chang (1996) initially reported a lack of hepatic NcoA4 mRNA expression, but this inconsistency is probably explained by the use of Northern blot analysis, which is less sensitive than RT-PCR.

The tissue distribution of NcoA4 suggests potential widespread actions of NcoA4 during development. By altering AR and AhR function, NcoA4 could participate in tissue differentiation and function. In addition to affecting sexual differentiation and function of the male reproductive tract, androgens have been implicated in cardiac and lung development. AR-null mice have reduced heart size, as compared with wild-type controls, and have an increased susceptibility to fibrosis induced by angiotensin II treatment (Ikeda et al. 2005), indicating that AR mediates growth-promoting and protective effects of androgens in cardiac cells.

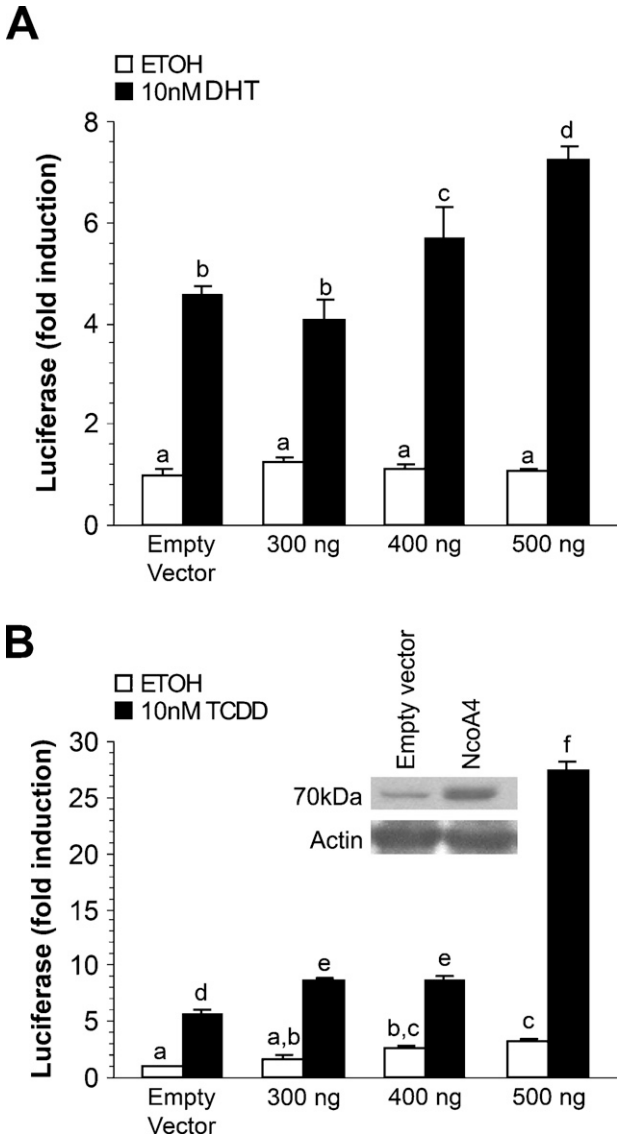

Figure 10 Effect of mNcoA4 on androgen receptor (AR)-mediated or aryl hydrocarbon receptor (AhR)-mediated transactivation in COS cells. COS cells were transiently transfected with expression vectors for NcoA4 and AR (**A**) or AhR (**B**). Cells were treated with vehicle (ethanol or *n*-nonane) or 10 nM dihydrotestosterone or 10 nM 2,3,7,8-tetrachlorodibenzo-*p*-dioxin 24 hr after transfection and were harvested 24 hr after treatment. Shown is a representative graph of one of three experiments. Bars represent the mean ± SEM of three replicates. Bars with different letters are statistically different from one another as determined by ANOVA followed by a Fisher's least-significant difference post-hoc test ($p<0.05$).

Figure 9 NcoA4 protein distribution in various adult mouse tissues. Tissue distribution of NcoA4 protein on paraffin-embedded adult mouse tissue sections was determined by immunohistochemistry using anti-NcoA4 goat (Q19) polyclonal antibody. All sections were counterstained with hematoxylin. The staining pattern was similar to that found with H300 rabbit polyclonal antibody (Figure 8). Staining with normal goat serum substituted for primary antibody was used as negative control for all tissues examined. Bar = 60 μm.

Androgens acting through the AR in cardiomyocytes have been shown to produce cardiac hypertrophy (Marsh et al. 1998). Androgens have also been implicated in delaying male lung development, an effect that may involve opposing the actions of epidermal growth factor signaling (Klein and Nielsen 1993).

However, our data indicate that murine NcoA4 is a more potent coactivator for AhR than for AR, with NcoA4 overexpression increasing AR-dependent luciferase expression only slightly. In contrast, NcoA4 enhanced AhR transcriptional activity by up to 5-fold. AhR appears to be involved in early mouse embryo development and is expressed ubiquitously after E9.5 in different embryonic tissues, including liver, lung, heart, and bone (Abbott et al. 1995; Jain et al. 1998). AhR-null mice exhibit lower growth rates and peripheral immune system deficiency (Gonzalez et al. 1995; Fernandez-Salguero et al. 1997). AhR signaling in hepatocytes is involved in adaptive metabolism and dioxin toxicity, whereas signaling in hematopoietic cells is involved in the closure of the ductus venosus (Walisser et al. 2005). AhR-null mice develop progressive cardiac hypertrophy and fibrosis (Gonzalez et al. 1995; Fernandez-Salguero et al. 1997; Lund et al. 2006), as well as an increased incidence of fibrotic lung lesions (Gonzalez et al. 1995; Fernandez-Salguero et al. 1997). Interestingly, a recent study in human prostate cancer and benign tumor samples indicates that NcoA4 expression is regulated by a member of the developmentally important, high-mobility group box–containing transcription factor, Sox4 (Liu et al. 2006). Sox4-null mice die at E14 as a result of cardiac defects (Schilham et al. 1996; Ya et al. 1998). Further studies are required to determine the role of NcoA4 in development.

In summary, our results demonstrate a dynamic expression profile for NcoA4 during early development, particularly in cardiac, hepatic, and lung tissue and indicate that murine NcoA4 is a potent modulator of AhR activity. These findings suggest that this coactivator may play an important role in modulating nuclear receptor activity during development and/or organogenesis. Future studies in which NcoA4 expression is disrupted in specific murine tissues are required to determine the developmental and functional roles of this coactivator.

Acknowledgments

This work was supported by a grant from the Natural Sciences and Engineering Research Council of Canada.

Literature Cited

Abbott BD, Birnbaum LS, Perdew GH (1995) Developmental expression of two members of a new class of transcription factors: I. Expression of aryl hydrocarbon receptor in the C57BL/6N mouse embryo. Dev Dyn 204:133–143

Alen P, Claessens F, Schoenmakers E, Swinnen JV, Verhoeven G, Rombauts W, Peeters B (1999) Interaction of the putative androgen receptor-specific coactivator ARA70/ELE1alpha with multiple steroid receptors and identification of an internally deleted ELE1beta isoform. Mol Endocrinol 13:117–128

Amazit L, Alj Y, Tyagi RK, Chauchereau A, Loosfelt H, Pichon C, Pantel J, et al. (2003) Subcellular localization and mechanisms of nucleocytoplasmic trafficking of steroid receptor coactivator-1. J Biol Chem 278:32195–32203

Amazit L, Pasini L, Szafran AT, Berno V, Wu RC, Mielke M, Jones ED, et al. (2007) Regulation of SRC-3 intercompartmental dynamics by estrogen receptor and phosphorylation. Mol Cell Biol 27:6913–6932

Crocoll A, Zhu CC, Cato AC, Blum M (1998) Expression of androgen receptor mRNA during mouse embryogenesis. Mech Dev 72:175–178

Evangelou A, Jindal SK, Brown TJ, Letarte M (2000) Down-regulation of transforming growth factor beta receptors by androgen in ovarian cancer cells. Cancer Res 60:929–935

Fernandez-Salguero PM, Ward JM, Sundberg JP, Gonzalez FJ (1997) Lesions of aryl-hydrocarbon receptor-deficient mice. Vet Pathol 34:605–614

Gao T, Brantley K, Bolu E, McPhaul MJ (1999) RFG (ARA70, ELE1) interacts with the human androgen receptor in a ligand-dependent fashion, but functions only weakly as a coactivator in cotransfection assays. Mol Endocrinol 13:1645–1656

Gonzalez FJ, Fernandez-Salguero P, Lee SS, Pineau T, Ward JM (1995) Xenobiotic receptor knockout mice. Toxicol Lett 82–83: 117–121

He B, Minges JT, Lee LW, Wilson EM (2002) The FXXLF motif mediates androgen receptor-specific interactions with coregulators. J Biol Chem 277:10226–10235

Heinlein CA, Chang C (2002) Androgen receptor (AR) coregulators: an overview. Endocr Rev 23:175–200

Heinlein CA, Chang C (2003) Induction and repression of peroxisome proliferator-activated receptor alpha transcription by coregulator ARA70. Endocrine 21:139–146

Heinlein CA, Ting HJ, Yeh S, Chang C (1999) Identification of ARA70 as a ligand-enhanced coactivator for the peroxisome proliferator-activated receptor gamma. J Biol Chem 274:16147–16152

Hu YC, Yeh S, Yeh SD, Sampson ER, Huang J, Li P, Hsu CL, et al. (2004) Functional domain and motif analyses of androgen receptor coregulator ARA70 and its differential expression in prostate cancer. J Biol Chem 279:33438–33446

Ikeda Y, Aihara K, Sato T, Akaike M, Yoshizumi M, Suzaki Y, Izawa Y, et al. (2005) Androgen receptor gene knockout male mice exhibit impaired cardiac growth and exacerbation of angiotensin II-induced cardiac fibrosis. J Biol Chem 280:29661–29666

Jain S, Maltepe E, Lu MM, Simon C, Bradfield CA (1998) Expression of ARNT, ARNT2, HIF1 alpha, HIF2 alpha and Ah receptor mRNAs in the developing mouse. Mech Dev 73:117–123

Jost A, Gonse-Danysz P, Jacquot R (1953) [Studies on physiology of fetal hypophysis in rabbits and its relation to testicular function.] J Physiol (Paris) 45:134–136

Keller ET, Ershler WB, Chang C (1996) The androgen receptor: a mediator of diverse responses. Front Biosci 1:d59–71

Klein JM, Nielsen HC (1993) Androgen regulation of epidermal growth factor receptor binding activity during fetal rabbit lung development. J Clin Invest 91:425–431

Kollara A, Brown TJ (2006) Functional interaction of nuclear receptor coactivator 4 with aryl hydrocarbon receptor. Biochem Biophys Res Commun 346:526–534

Kollara A, Brown TJ (2009) Modulation of aryl hydrocarbon receptor activity by four and a half LIM domain 2. Int J Biochem Cell Biol 41:1182–1188

Kollara A, Kahn HJ, Marks A, Brown TJ (2001) Loss of androgen receptor associated protein 70 (ARA70) expression in a subset of HER2-positive breast cancers. Breast Cancer Res Treat 67:245–253

Lanzino M, De Amicis F, McPhaul MJ, Marsico S, Panno ML, Ando S (2005) Endogenous coactivator ARA70 interacts with estrogen receptor alpha (ERalpha) and modulates the functional ERalpha/

androgen receptor interplay in MCF-7 cells. J Biol Chem 280: 20421–20430

Liu P, Ramachandran S, Ali Seyed M, Scharer CD, Laycock N, Dalton WB, Williams H, et al. (2006) Sex-determining region Y box 4 is a transforming oncogene in human prostate cancer cells. Cancer Res 66:4011–4019

Lund AK, Goens MB, Nunez BA, Walker MK (2006) Characterizing the role of endothelin-1 in the progression of cardiac hypertrophy in aryl hydrocarbon receptor (AhR) null mice. Toxicol Appl Pharmacol 212:127–135

Magklara A, Brown TJ, Diamandis EP (2002) Characterization of androgen receptor and nuclear receptor co-regulator expression in human breast cancer cell lines exhibiting differential regulation of kallikreins 2 and 3. Int J Cancer 100:507–514

Marsh JD, Lehmann MH, Ritchie RH, Gwathmey JK, Green GE, Schiebinger RJ (1998) Androgen receptors mediate hypertrophy in cardiac myocytes. Circulation 98:256–261

Mestayer C, Blanchere M, Jaubert F, Dufour B, Mowszowicz I (2003) Expression of androgen receptor coactivators in normal and cancer prostate tissues and cultured cell lines. Prostate 56: 192–200

Rahman MM, Miyamoto H, Takatera H, Yeh S, Altuwaijri S, Chang C (2003) Reducing the agonist activity of antiandrogens by a dominant-negative androgen receptor coregulator ARA70 in prostate cancer cells. J Biol Chem 278:19619–19626

Sambrook J, Russell DW (2001) Molecular Cloning: A Laboratory Manual. 3rd ed. Cold Spring Harbor, NY, Cold Spring Harbor Laboratory Press

Sasaki K, Matsumura G (1986) Haemopoietic cells of yolk sac and liver in the mouse embryo: a light and electron microscopical study. J Anat 148:87–97

Schilham MW, Oosterwegel MA, Moerer P, Ya J, de Boer PA, van de Wetering M, Verbeek S, et al. (1996) Defects in cardiac outflow tract formation and pro-B-lymphocyte expansion in mice lacking Sox-4. Nature 380:711–714

Shaw PA, Rittenberg PV, Brown TJ (2001) Activation of androgen receptor-associated protein 70 (ARA70) mRNA expression in ovarian cancer. Gynecol Oncol 80:132–138

Siriett V, Nicholas G, Berry C, Watson T, Hennebry A, Thomas M, Ling N, et al. (2006) Myostatin negatively regulates the expression of the steroid receptor co-factor ARA70. J Cell Physiol 206: 255–263

Thin TH, Kim E, Yeh S, Sampson ER, Chen YT, Collins LL, Basavappa R, et al. (2002) Mutations in the helix 3 region of the androgen receptor abrogate ARA70 promotion of 17beta-estradiol-induced androgen receptor transactivation. J Biol Chem 277:36499–36508

Ting HJ, Bao BY, Hsu CL, Lee YF (2005) Androgen-receptor coregulators mediate the suppressive effect of androgen signals on vitamin D receptor activity. Endocrine 26:1–9

Walisser JA, Glover E, Pande K, Liss AL, Bradfield CA (2005) Aryl hydrocarbon receptor-dependent liver development and hepatotoxicity are mediated by different cell types. Proc Natl Acad Sci USA 102:17858–17863

Xu J, Li Q (2003) Review of the in vivo functions of the p160 steroid receptor coactivator family. Mol Endocrinol 17:1681–1692

Ya J, Schilham MW, de Boer PA, Moorman AF, Clevers H, Lamers WH (1998) Sox4-deficiency syndrome in mice is an animal model for common trunk. Circ Res 83:986–994

Yeh S, Chang C (1996) Cloning and characterization of a specific coactivator, ARA70, for the androgen receptor in human prostate cells. Proc Natl Acad Sci USA 93:5517–5521

Zhou ZX, He B, Hall SH, Wilson EM, French FS (2002) Domain interactions between coregulator ARA(70) and the androgen receptor (AR). Mol Endocrinol 16:287–300

The Journal of Histochemistry & Cytochemistry